

Modeling of carbon nanotube Schottky barrier modulation under oxidizing conditions

Toshishige Yamada*

NASA Ames Research Center, M/S 229-1, Moffett Field, California 94035-1000, USA

(Received 10 June 2003; revised manuscript received 2 September 2003; published 18 March 2004; corrected 1 April 2004)

A model is proposed for the previously reported lower Schottky barrier Φ_{Bh} for hole transport in air than in vacuum at a junction between the metallic electrode and semiconducting carbon nanotube (CNT). We consider the electrostatics in a transition region between the electrode and CNT in the presence or absence of oxygen molecules (air or vacuum), where an appreciable potential drop occurs. The role of oxygen molecules is to increase this potential drop with a negative oxygen charge, leading to lower Φ_{Bh} in air. The Schottky barrier modulation is large when a CNT depletion mode is involved, while the modulation is negligible when a CNT accumulation mode is involved. The mechanism prevails in both *p*- and *n*-CNT's, and the model consistently explains the key experimental findings.

DOI: 10.1103/PhysRevB.69.125408

PACS number(s): 73.30.+y, 85.35.Kt, 81.16.Pr

I. INTRODUCTION

The effects of carbon nanotube (CNT) oxidation have been studied in thermopower experiments, and it has been found that the thermoelectric power coefficient was negative in vacuum and positive in air.¹ In fact, the thermoelectric power coefficient indicates how a bulk internal electric field is created in order to counterbalance the bulk carrier flow due to the thermal gradient, and it characterizes the *bulk* properties.² Thus oxidation changes the *bulk* CNT properties.

Recently, oxidation effects have been studied³ using CNT field-effect transistors⁴ (FET's), and it has been shown that the *contact* properties at the electrode and CNT are modified in oxidation. The CNT was placed on a silicon dioxide layer, and a gate voltage V_G was applied to the doped silicon substrate (backgate) as schematically shown in Fig. 1(a). The CNT was about 1 μm long, and the source and drain gold electrodes covered about one-third of the CNT, respectively. The channel length was a few tenths of a micrometer. They measured the drain current I_D as a function of V_G and the drain voltage V_D , and estimated the channel conductance $g_d = \partial I_D(V_G, V_D) / \partial V_D$. The role of V_G was to change the CNT doping effectively or modulate the Fermi level. With the application of V_G , positive and negative charges were introduced as shown in Fig. 1(a). The electric field under the source and drain electrodes was mostly vertical due to the thin CNT and wide electrode geometry. In this situation, the planar junction theory is applicable.^{5,6} The CNT conduction- and valence-band edges have the shape shown in Fig. 1(b) along the arrow path in Fig. 1(a), where A–D indicate spatial points in the structure. The path and electric field are parallel only at the CNT ends, and band bending occurs only there. V_G determines this field strength and, therefore, the amount of band bending. Thus V_G effectively changes the CNT doping and modifies the Fermi level by αV_G , where α is related to the oxide capacitance and CNT capacitance.^{6,7} α is usually on the order of 10^{-1} in experiments,^{3,4} meaning that only a portion of V_G is reflected in the Fermi level change.

In this experimental setup, g_d was observed to rise slowly at a negative $V_G(V_{G1})$ and rapidly at a positive $V_G(V_{G2})$ in

vacuum as indicated in Fig. 2(a). In air, the g_d asymmetry flipped: g_d rose rapidly at a negative $V_G(V_{G3})$ and slowly at a positive $V_G(V_{G4})$ as shown in Fig. 2(b). This was attributed to the contact property change of the electrode and CNT (Ref. 3): at $V_G=0$, the Schottky barrier for holes (Φ_{Bh}) was high and that for electrons (Φ_{Be}) was low in vacuum [Fig. 2(c)], while Φ_{Bh} was low and Φ_{Be} was high in air [Fig. 2(d)]. Then g_d rose slowly at V_{G1} , since the holes started to tunnel through a high Φ_{Bh} [Fig. 2(e)], and g_d rose rapidly at V_{G2} , since electrons started to tunnel through low Φ_{Be} [Fig. 2(f)]. Similarly, g_d rose rapidly at V_{G3} because of low Φ_{Bh} [Fig. 2(g)], and g_d rose slowly at V_{G4} because of high Φ_{Be} [Fig. 2(h)]. In this g_d - V_G experiment, the *contact* property modulation of the CNT in oxidation was much more influential than the *bulk* property change,⁸ and the experimental findings were consistently explained through the Schottky barrier modulation.

However, the standard Schottky (no pinning) theory^{5,9–12} does not explain this Schottky barrier modulation. In that theory, we must consider the system as a junction of an oxidized metallic electrode surface and a plain CNT or as a plain metallic electrode and an oxidized CNT, and align the bands at the contact. Usually, a gold surface is inert, thus insensitive to oxidation, so the first description is not appropriate. The second description turns out to give a qualitatively wrong result as discussed now. Generally, a negative charge at the material surface will *increase* the surface dipole

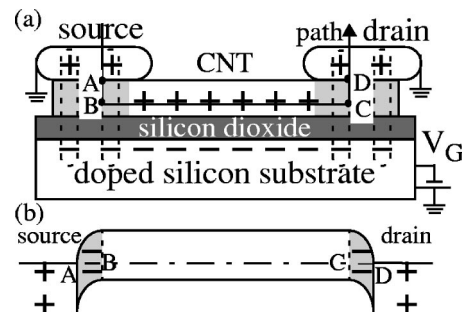


FIG. 1. CNT FET with gate voltage V_G in equilibrium ($V_D = 0$): (a) real-space charge distribution and (b) equivalent band structure along the arrow path above, where A–D indicate corresponding points from (a).

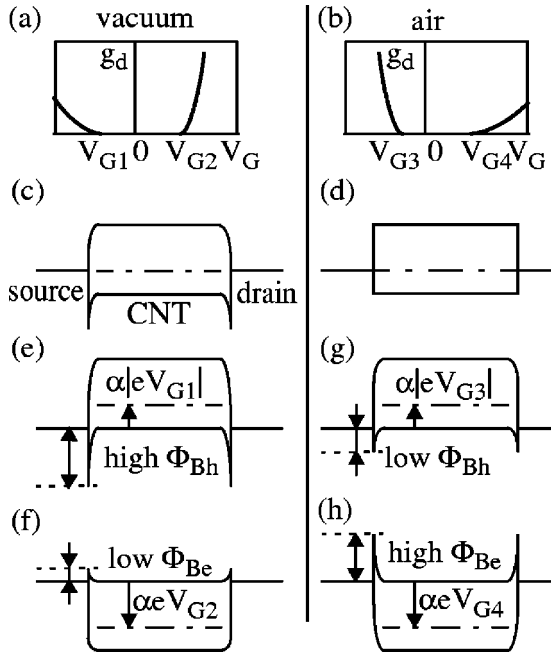


FIG. 2. CNT FET g_d - V_G characteristics and band structures with $V_D=0$: (a) g_d - V_G characteristics in vacuum, (b) g_d - V_G characteristics in air, (c) band structure in vacuum at $V_G=0$, (d) band structure in air at $V_G=0$, (e) band structure at V_{G1} in vacuum, (f) band structure at V_{G2} in vacuum, (g) band structure at V_{G3} in air, and (h) band structure at V_{G4} in air.

and further confine the electrons within the material.⁹ Electronegative oxygen molecules are negatively charged, so the CNT electron affinity ϕ'_s in air should *increase* from ϕ_s in vacuum such that $\phi'_s > \phi_s$. (Throughout this article, we use the convention that a prime indicates a quantity in air.) Figures 3(a)–3(d) represent band structures across the electrode-CNT junction. The CNT conduction- and valence-band edges are shown with the Fermi level ζ , and χ_m is the work function of the metallic electrode. According to standard Schottky theory, we match the tops of χ_m and ϕ_s at the interface as shown in Figs. 3(a) and 3(b). Then Φ_{Bh} in vacuum and Φ'_{Bh} in air are expressed by

$$\Phi_{Bh} = E_G + \phi_s - \chi_m, \quad (1)$$

$$\Phi'_{Bh} = E_G + \phi'_s - \chi_m. \quad (2)$$

Thus $\Phi_{Bh} < \Phi'_{Bh}$, but this contradicts the experimental observations described above. In Schottky theory, all oxidation effects are represented in the modulated work function ϕ'_s . It is clear that the Schottky theory does not explain the experiment consistently.

We will propose a model to overcome this difficulty and explain the Schottky barrier modulation consistently. Our model is related to the Bardeen theory regarding surface states.^{9–12} We will consider the electrostatic charge balance¹⁰ inside the Schottky junction, while this degree of freedom is not incorporated in the traditional concept of an “intimate Schottky junction” in Schottky theory. We will first demon-

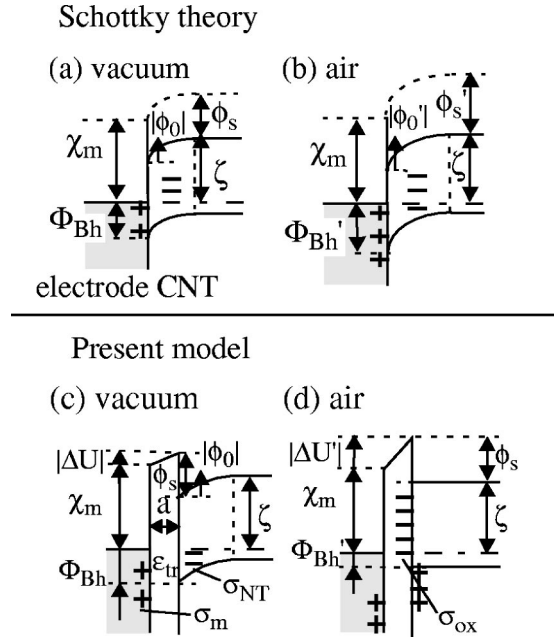


FIG. 3. Band structures for a Schottky junction between the metallic electrode and semiconducting CNT (a) in vacuum and (b) in air based on the conventional view of an intimate contact, resulting in the incorrect relation of low Schottky barrier for holes in vacuum Φ_{Bh} and high Schottky barrier for holes in air Φ'_{Bh} ; proposed band structures (c) in vacuum and (d) in air showing a potential drop ΔU in the transition region, resulting in the correct relation of $\Phi_{Bh} > \Phi'_{Bh}$. Here a is the transition region width, ϵ_{tr} is the dielectric constant, ϕ_s is the CNT electron affinity, ζ is the CNT Fermi level, χ_m is the metallic work function, Φ_{Bh} is the hole Schottky barrier, and σ_{ox} is the negative charge due to oxygen molecules.

strate that our model certainly predicts a correct Schottky barrier modulation using energy band structures in Sec. II and then present a detailed mathematical formulation in Sec. III. The analytical solutions are given in the Appendix. The relevant equations are solved graphically to develop an intuitive understanding, and four different types of Schottky barrier modulations are discussed in Sec. IV. Experiments in Ref. 3 are examined using our model in Sec. V, and a summary is given in Sec. VI.

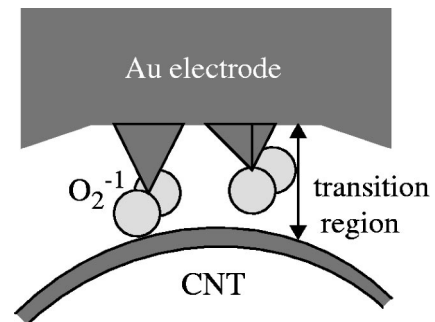


FIG. 4. Schematic view of the transition region in the gold-electrode – CNT interface, where gold clusters are formed and oxygen molecules are chemisorbed on top of the clusters.

II. SCHOTTKY BARRIER MODULATION MECHANISM

We consider here that the Schottky junction has a sandwich structure as shown in Fig. 4: a gold bulk electrode, gold clusters at the electrode surface, charged oxygen molecules, and the CNT surface. The region between the bulk electrode and CNT is called the “transition region.” In fact, a deposited gold surface has bumps with a width on the order of $10^{-1} \mu\text{m}$ (Ref. 13), and oxygen molecules can move into the gaps of the transition region (interface between electrode and CNT). Moreover, the electrode surface facing the CNT is expected to be microscopically (on the order of several angstroms) rough, since during the electrode deposition process, gold atoms are attracted by the CNT (Ref. 14) and tend to form clusters. Although the microscopically flat gold surface is known to be inert to oxygen molecules, the clusters on the gold surface can chemisorb oxygen molecules at their tips and form $\text{O}_2^{-1}/\text{Au}_n/\text{Au}(111)$ with an n -dependent binding energy ranging from ~ 0.45 to ~ 0.96 eV ($n=1-3$) (Ref. 15). These gold clusters have the highest occupied molecular orbitals (HOMO's), and these orbitals are localized with their charge densities sticking out into the vacuum. Oxygen molecules bind to these sites. In each cluster, a charge transfer occurs from the gold HOMO to the oxygen π^* orbital, and the oxygen molecule becomes negatively charged. The microscopically flat gold surfaces do not have these localized HOMO's and are inert to oxygen molecules. Thus the presence of the CNT is critical for cluster formation and oxygen chemisorption on the gold electrode surface.

There are also discussions in the literature about interactions between oxygen molecules and the CNT. Some researchers have predicted physisorption of oxygen molecules on the CNT with negligible charge transfer,¹⁶ while others have predicted chemisorption of oxygen molecules on the CNT and estimated the transferred charge to be -0.1 with a binding energy of ~ 0.25 eV (Ref. 17). In either case, the oxygen molecules dominantly interact with the gold surface clusters and are negatively charged by -1 , regardless of whether the electrode and CNT are in an open- or closed-circuit condition.

The difference between the open- and closed-circuit conditions will appear in the distribution of the positive charge (which balances the oxygen's negative charge). Under open-circuit conditions, the positive charge will appear mostly in the electrode, reflecting the dominant gold-oxygen interaction. However, under the closed-circuit conditions with $V_D = 0$, which is our case, the positive charge will move within the circuit and appear in both the electrode and CNT. This is how the system keeps the Fermi level constant everywhere. Once the circuit is closed, the distribution of the positive charge is determined by the electrostatics in the transition region, rather than the details of the oxygen-gold or oxygen-CNT interactions. We will study how the negative oxygen charge and resulting positive charge in the transition region modify the Schottky barrier under the closed-circuit condition.¹⁸

The key conclusion is that the potential drop ΔU in the transition region is modified by oxidation. The negatively charged oxygen molecules will induce a balancing positive

charge in the electrode and CNT, and ΔU will be modified. As will be shown in the following section, $|\Delta U|$ turns out to be small in vacuum and large in air. This will, in fact, lead to a correct Schottky barrier behavior consistent with the experiments in Ref. 3. We will show this with a p -CNT, but the same mechanism will also work for an n -CNT. For the two cases where $|\Delta U|$ is small in vacuum or large in air, the system has band structures as shown in Figs. 3(c) and 3(d), respectively. Thus we have Φ_{Bh} in vacuum and Φ'_{Bh} in air:

$$\Phi_{Bh} = \phi_s + E_G - \chi_m - |\Delta U|, \quad (3)$$

$$\Phi'_{Bh} = \phi_s + E_G - \chi_m - |\Delta U'|. \quad (4)$$

This time, $|\Delta U| < |\Delta U'|$ and $\Phi_{Bh} > \Phi'_{Bh}$, which is consistent with the experiments. χ_m is the work function for the plain metallic surface and ϕ_s is the electron affinity for the plain CNT surface. We use the free bulk material parameters ϕ_s and χ_m in Eqs. (3) and (4), and all oxidation effects are included in ΔU .

The difference between the standard Schottky theory^{5,9-12} and our model is well represented in the band structures: ΔU is absent in the former as shown in Figs. 3(a) and 3(b), while ΔU is present and is significantly modified in oxidation in the latter as shown in Figs. 3(c) and 3(d). In the Schottky theory, Φ_{Bh} is determined by the bulk properties only, through ϕ_s and χ_m . In our model, Φ_{Bh} is determined by the potential drop ΔU in the transition region reflecting the contact properties, in addition to the bulk properties ϕ_s and χ_m . We will see in the next section that our model actually includes the standard Schottky theory as a special limit of vanishing transition layer width.

III. MATHEMATICAL FORMULATION

Now we will study how the potential drop ΔU is modulated in oxidation in our model. For this purpose, we will derive a relation for the CNT band bending ϕ_0 and ΔU at a fixed V_G based on the charge-neutrality relation¹⁰ within the planar junction theory^{5,12} under the closed-circuit condition. The negative oxygen charge σ_{ox} per unit area is independent of the Fermi level ζ and is constant. There is a charge σ_m per unit area on the metallic electrode surface and a charge σ_{NT} per unit area within the CNT in the depletion or accumulation mode. The charge-neutrality relation requires

$$\sigma_m + \sigma_{ox} + \sigma_{NT} = 0. \quad (5)$$

That is, the positive countercharges σ_m and σ_{NT} must neutralize the negative σ_{ox} . Mathematically, this is equivalent to determining the CNT band bending ϕ_0 for a given σ_{ox} . Then we would know how the positive charge divides between σ_m and σ_{NT} . Analytical solutions of this problem are presented in the Appendix. Here we will provide graphical solutions to develop an intuitive understanding. The charge-neutrality condition can be split into two equations

$$\sigma = -\sigma_m(\phi_0) = \Delta U \epsilon_{tr} / ea = [\chi_m - (\phi_s + \phi_0 + \zeta)] \epsilon_{tr} / ea, \quad (5a)$$

$$\sigma = \sigma_{NT}(\phi_0) + \sigma_{ox}, \quad (5b)$$

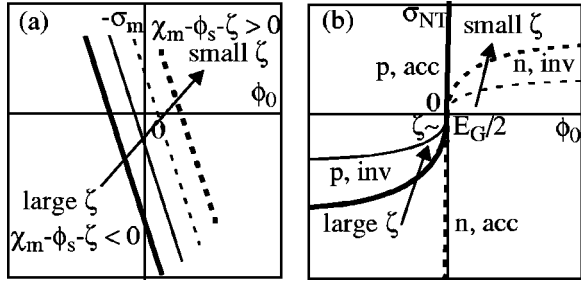


FIG. 5. General shape of the charge functions: (a) $\sigma = -\sigma_m(\phi_0)$ and (b) $\sigma = -\sigma_{NT}(\phi_0) + \sigma_{ox}$ with $\sigma_{ox} = 0$. Arrow indicates the curve movement for changing V_G from negative to positive, which causes a transition from p -CNT to n -CNT.

where ϵ_{tr} is an effective dielectric constant for the transition region (an appropriate average including the vacuum, gold clusters, and oxygen molecules, as discussed in Sec. V), a is the width of the transition region, and e is the unit charge.¹⁹ After specifying the system including the oxidation level, we know the functional forms of $\sigma = -\sigma_m(\phi_0)$ and $\sigma = \sigma_{NT}(\phi_0) + \sigma_{ox}$ for a given value of σ_{ox} . The intersection of these, Eqs. (5a) and (5b), defines ϕ_0 and σ . Here σ determines ΔU through Eq. (5a). Then we calculate Φ_{Bh} by

$$\Phi_{Bh} = \phi_s + E_G - \chi_m + \Delta U. \quad (6)$$

This is an extension of Eq. (3) and can be used for both positive and negative ΔU . The gate voltage V_G appears as a modulation of the Fermi level ζ by²⁰

$$\zeta = \zeta(V_G) = \zeta_0 - \alpha V_G, \quad (7)$$

where ζ_0 is a value at $V_G = 0$. In our definition, ζ is measured from the bottom of the conduction band as in Figs. 3(c) and 3(d), rather than from the top of the valence band. A negative V_G will increase the hole density and therefore increase ζ , while a positive V_G will increase the electron density and therefore decrease ζ .

We will discuss the general shape of $\sigma = -\sigma_m(\phi_0)$ depending on whether the metallic work function χ_m is smaller or larger than the CNT work function $\phi_s + \zeta$. When $\chi_m < \phi_s + \zeta$, because of a shallow metallic work function χ_m or a large Fermi level ζ at a large negative V_G , $\sigma = -\sigma_m(\phi_0)$ is as shown by the thick (largest $\zeta \sim E_G$) or thin (large ζ) solid line with a negative slope, intersecting with the negative ϕ_0 axis in Fig. 5(a). This is simply a standard charge-voltage relation for a capacitor. Only when $\chi_m = \phi_s + \phi_0 + \zeta$ or the CNT band bending ϕ_0 exactly compensates the work function difference $\chi_m - (\phi_s + \zeta)$ do we have $\sigma_m = 0$. Otherwise, we have a finite σ_m and therefore a finite ΔU . The same functional form of Eq. (5a) can be used for both p - and n -CNT's. When $\chi_m > \phi_s + \zeta$, because of a deep metallic work function χ_m or a small Fermi level ζ at a large positive V_G , $\sigma = -\sigma_m(\phi_0)$ is as shown by the thin (small ζ) or thick (smallest $\zeta \sim 0$) dashed line with a negative slope, intersecting with the positive ϕ_0 axis in Fig. 5(a). If we change V_G from negative to positive and modify the CNT from p type to n type, ζ decreases monotonically from $\sim E_G$ to ~ 0 , and σ

$= -\sigma_m(\phi_0)$ will shift upward as the arrow indicates, from thick solid, to thin solid, to thin dashed, to thick dashed line.

Next, we will discuss the general shape of $\sigma = \sigma_{NT}(\phi_0) + \sigma_{ox}$ for $\sigma_{ox} = 0$. In fact, a finite negative σ_{ox} simply shifts the entire curve downward, so the discussion can be limited to $\sigma_{ox} = 0$ without loss of generality. In the p -CNT case, accumulation occurs for $\phi_0 > 0$, and $\sigma = \sigma_{NT}(\phi_0)$ is positive and increases very rapidly with ϕ_0 . Depletion occurs for $\phi_0 < 0$, and $\sigma = \sigma_{NT}(\phi_0) = -(2\epsilon_{NT}|\phi_0|N_B)^{1/2}$ is negative and has the shape of a parabola, based on planar junction theory,⁵ where N_B is the effective CNT background (three-dimensional) charge density determined by ζ and therefore by V_G through Eq. (7). Thus $\sigma = \sigma_{NT}(\phi_0)$ for p -CNT follows the thick (largest $\zeta \sim E_G$, large N_B) or thin (large ζ , small N_B) solid curve in Fig. 5(b). In the n -CNT case, accumulation occurs for $\phi_0 < 0$, and $\sigma = \sigma_{NT}(\phi_0)$ is negative and decreases very rapidly with decreasing ϕ_0 . Depletion occurs for $\phi_0 > 0$, and $\sigma = \sigma_{NT}(\phi_0) = +(2\epsilon_{NT}\phi_0 N_B)^{1/2}$ is positive and has the shape of a parabola. Thus $\sigma = \sigma_{NT}(\phi_0)$ for n -CNT follows the thin (small ζ , small N_B) or thick (smallest $\zeta \sim 0$, large N_B) dashed curve in Fig. 5(b). If we change V_G from negative to positive and modify the CNT from p type to n type, ζ decreases monotonically from $\sim E_G$ to ~ 0 . Thus the curve will change as the arrow indicates, from thick solid, to thin solid, to thin dashed, to thick dashed curve. When $\zeta \sim E_G/2$ and the CNT is almost intrinsic, the curve approaches the horizontal axis $\sigma = 0$, since the band bending ϕ_0 does not produce any appreciable charge σ in the CNT. Inversion will occur for large $|\phi_0|$, but the intersections of interest in this case occur in the accumulation and depletion portions. The inversion onsets are not shown in the figure.

In the standard Schottky theory,^{5,9-12} the relation $\chi_m = \phi_s + \phi_0 + \zeta$ is assumed *a priori*. Mathematically, our model includes standard Schottky theory as a special limiting case of vanishing transition region width $a \rightarrow 0$. Then $\epsilon_{tr}/ea \rightarrow \infty$ and the relation $\chi_m = \phi_s + \phi_0 + \zeta$ must hold to avoid the divergence on the right-hand side of Eq. 5(a). Physically, this means that the CNT band bending ϕ_0 exactly compensates the work function difference $\chi_m - (\phi_s + \zeta)$ when $a \rightarrow 0$. In this limit, to achieve electrostatic balance within the Schottky junction by neutralizing the oxygen molecule charge σ_{ox} , a degree of freedom is removed from our model, and ϕ_0 is determined only by the properties of the bulk farther away from the junction. The right-hand side of Eq. (5a) has the form of $0 \times \infty$ and the metallic charge σ_m is uncertain. Graphically, the solution of Eq. (5a) is almost vertical, and the intersection of Eqs. (5a) and (5b) is uncertain, or its location can be anywhere on the σ axis. This uncertainty leaves room for the concept of modified bulk parameters in oxidation, but as we have already seen with a band structure scheme, this approach is physically inappropriate and will lead to contradictory results. The explicit inclusion of a finite σ_{ox} in the transition region with a finite a as we have done in our model is essential in explaining the experimental observations.³

IV. FOUR SCHOTTKY BARRIER MODULATIONS

Depending on whether the CNT is p type or n type and on whether the metallic work function χ_m is smaller or larger

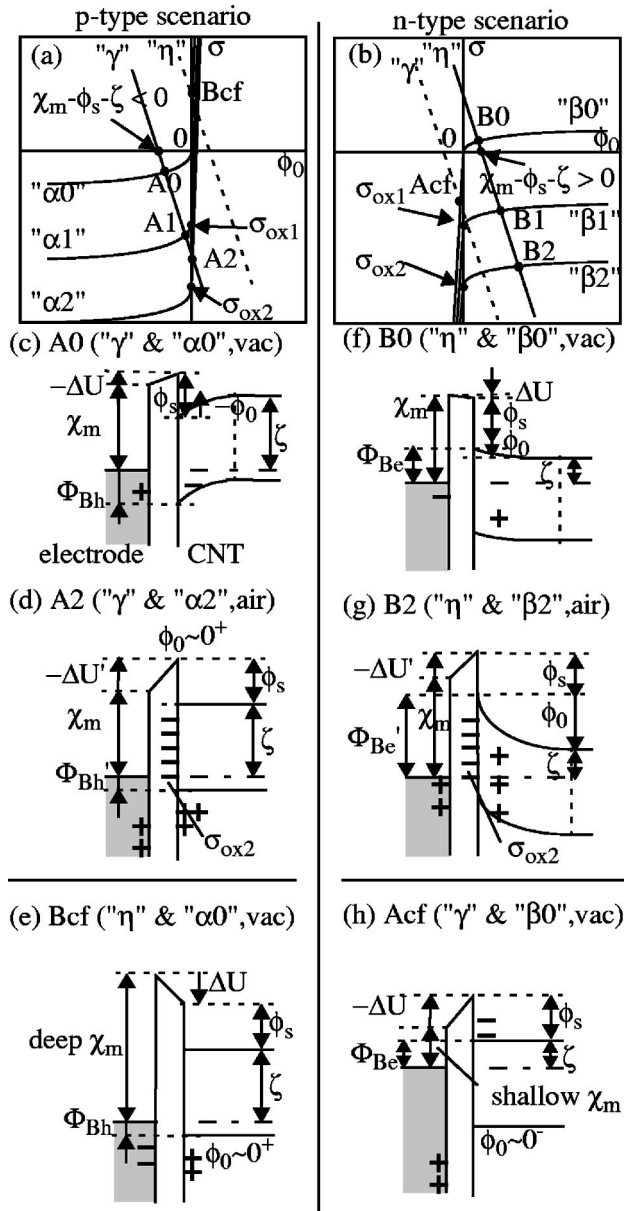


FIG. 6. Graphical solution of our model by finding the intersections of a metallic electrode charge line “ γ ” or “ η ” and a charge curve “ α_i ” or “ β_i ” ($i=0, 1, \text{ or } 2$) for the CNT and oxygen molecules as a function of band bending ϕ_0 . Here “ γ ” is for $\chi_m < \phi_s + \zeta$, and “ η ” is for $\chi_m > \phi_s + \zeta$, where χ_m is the metallic electrode work function, ϕ_s is the CNT electron affinity, and ζ is the Fermi level. (a) is for the p -CNT case and (b) is for the n -CNT case. $i=0$ corresponds to vacuum (oxygen charge $\sigma_{ox}=0$), $i=1$ to weak oxidation (small negative σ_{ox}), and $i=2$ to strong oxidation (large negative σ_{ox}). Band structures are shown for the resulting operating points: (c) A0 for a p -CNT in vacuum and (d) A2 for a p -CNT in air, demonstrating the correct relation $\Phi_{Bh} > \Phi'_{Bh}$; (e) Bcf for a p -CNT in vacuum with extremely deep χ_m ; (f) B0 for an n -CNT in vacuum and (g) B1 for an n -CNT in air, demonstrating the correct relation $\Phi_{Be} < \Phi'_{Be}$; (h) Acf for an n -CNT in vacuum with an extremely shallow χ_m .

than the CNT work function $\phi_s + \zeta$, there are four different cases, as illustrated in Fig. 6.

(i) p -CNT when $\chi_m < \phi_s + \zeta$ (line “ γ ”). In vacuum, $\sigma = \sigma_{NT}(\phi_0) + \sigma_{ox}$ with $\sigma_{ox}=0$ is curve “ $\alpha 0$ ” in Fig. 6(a), and the intersection with line “ γ ” is A0. Here A0 has a large negative (downward) band bending ϕ_0 in the depletion mode and a small negative σ corresponding to a small negative (right up, left down) ΔU from Eq. (5). The band structure at A0 is shown in Fig. 6(c). As the oxidation progresses, σ_{ox} becomes more and more negative. $\sigma = \sigma_{NT}(\phi_0) + \sigma_{ox}$ shifts downward and forms curves “ $\alpha 1$ ” and “ $\alpha 2$,” and the intersection with line “ γ ” moves down as $A0 \rightarrow A1 \rightarrow A2$. In the weak oxidation (“ $\alpha 1$ ”) of $0 > \sigma_{ox} > [\chi_m - (\phi_s + \zeta)]\epsilon_{tr}/ea$, A1 has a small negative ϕ_0 in the depletion mode and a large negative σ corresponding to a large negative ΔU . In the strong oxidation (“ $\alpha 2$ ”) of $[\chi_m - (\phi_s + \zeta)]\epsilon_{tr}/ea > \sigma_{ox}$, A2 has a negligible $\phi_0 \sim 0^+$ (almost flatband) in the accumulation mode and the largest negative σ corresponding to the largest negative ΔU . The band structure at A2 is shown in Fig. 6(d). It is clear that Φ_{Bh} decreases appreciably in oxidation. Physically, a negative oxygen charge σ_{ox} reduces the negative dopant charge in the p -CNT to satisfy the charge-neutrality condition, leading to an appreciable band bending reduction. Once the oxidation reaches $\sigma_{ox} = [\chi_m - (\phi_s + \zeta)]\epsilon_{tr}/ea$, the p -CNT cannot reduce the negative dopant charge anymore. The p -CNT must provide a positive charge, and this is possible in the accumulation mode. The accumulation charge is ample, and the p -CNT can provide any necessary positive charge with negligible band bending. Therefore, in weak oxidation where $0 > \sigma_{ox} > [\chi_m - (\phi_s + \zeta)]\epsilon_{tr}/ea$, the Schottky barrier modulation is significant. In strong oxidation where $[\chi_m - (\phi_s + \zeta)]\epsilon_{tr}/ea > \sigma_{ox}$, no further significant Schottky barrier modulation is expected.

(ii) p -CNT when $\chi_m > \phi_s + \zeta$ (line “ η ”). Line “ η ” intersects only at the accumulation portion of $\sigma = \sigma_{NT}(\phi_0) + \sigma_{ox}$, regardless of the value of σ_{ox} , as shown in Fig. 6(a). All intersections are of the Bcf type, in the first quadrant. The Bcf condition has a negligible $\phi_0 \sim 0^+$ and a large positive σ corresponding to a large positive ΔU . The band structure at Bcf is shown in Fig. 6(e). The p -CNT is consistently in the accumulation mode. Thus there is negligible change in ϕ_0 and ΔU , and the oxidation will not modify Φ_{Bh} practically. Physically, the metallic work function is so deep that the electrode charge must be negative and the CNT charge must be positive. The p -CNT is therefore locked into the accumulation mode and provides a positive charge. A negative oxygen charge σ_{ox} increases the already ample positive accumulation charge in the p -CNT to satisfy the charge-neutrality condition, but this is done without a practical change in the band bending. The Schottky barrier modulation is negligible.

(iii) n -CNT when $\chi_m > \phi_s + \zeta$ (line “ η ”). In vacuum, $\sigma = \sigma_{NT}(\phi_0) + \sigma_{ox}$ with $\sigma_{ox}=0$ is shown by curve “ $\beta 0$ ” in Fig. 6(b), and the intersection with line “ η ” is B0. Here B0 has a small positive ϕ_0 in the depletion mode and a small positive σ corresponding to a small positive ΔU . The band structure at B0 is shown in Fig. 6(f). As the oxidation progresses, $\sigma = \sigma_{NT}(\phi_0) + \sigma_{ox}$ shifts downward and forms curves “ $\beta 1$ ” and “ $\beta 2$,” and the intersection with line “ η ”

moves downward as $B0 \rightarrow B1 \rightarrow B2$. The n -CNT is locked into the depletion mode regardless of the value of σ_{ox} . Here $B2$ in the strong oxidation has a large positive ϕ_0 and a large negative σ corresponding to a large negative ΔU . The band structure at $B2$ is shown in Fig. 6(g). It is clear that Φ_{Be} increases appreciably in oxidation. Physically, a negative oxygen charge σ_{ox} requires more positive dopant charge in the n -CNT to satisfy the charge-neutrality condition, and this results in a further large positive band bending. The Schottky barrier modulation is significant.

(iv) n -CNT when $\chi_m < \phi_s + \zeta$ (line “ γ ”). In vacuum, the intersection with line “ γ ” occurs at the n -CNT accumulation portion of $\sigma = \sigma_{\text{NT}}(\phi_0) + \sigma_{\text{ox}}$, which corresponds to the Acf region in Fig. 6(b). In weak oxidation where $0 > \sigma_{\text{ox}} > [\chi_m - (\phi_s + \zeta)]\epsilon_{\text{tr}}/ea$, the intersection with line “ γ ” occurs at the accumulation portion consistently. The Acf condition has a negligible band bending $\phi_0 \sim 0^-$ and a large negative σ corresponding to a large negative ΔU . The band structure for the Acf condition is shown in Fig. 6(h). The band bending does not change substantially, and Φ_{Be} modulation is negligible. In strong oxidation where $[\chi_m - (\phi_s + \zeta)]\epsilon_{\text{tr}}/ea > \sigma_{\text{ox}}$, the n -CNT is in the depletion mode, and a finite positive ϕ_0 and a large negative σ are expected, leading to a finite increase in Φ_{Be} . Physically, the metallic work function is so shallow that the electrode charge must be positive and the n -CNT charge must be negative. A negative-charge σ_{ox} requires a decrease in the negative charge in the n -CNT to satisfy the charge-neutrality condition, and this requirement is met by reducing the n -CNT accumulation charge until $\sigma_{\text{ox}} = [\chi_m - (\phi_s + \zeta)]\epsilon_{\text{tr}}/ea$. Once σ_{ox} exceeds this limit, the n -CNT cannot reduce the accumulation charge further. The n -CNT must provide a positive charge, which is possible in the depletion mode. Thus a finite positive ϕ_0 results, and there is a finite Schottky barrier modulation. Therefore, in the weak-oxidation case of $0 > \sigma_{\text{ox}} > [\chi_m - (\phi_s + \zeta)]\epsilon_{\text{tr}}/ea$, the Schottky barrier modulation is negligible, but in the strong-oxidation case of $[\chi_m - (\phi_s + \zeta)]\epsilon_{\text{tr}}/ea > \sigma_{\text{ox}}$, a finite Schottky barrier modulation is expected.

V. DISCUSSION

As we have seen in Fig. 2, the Schottky barrier modulation due to oxidation was significant for both negative- and positive- V_G -bias conditions in Ref. 3. Thus we can exclude cases (ii) and (iv). The CNT was p type at the negative- V_G onset at V_{G1} in vacuum and at V_{G3} in air, and this should correspond to case (i). Then the condition $\chi_m < \phi_s + \zeta$ had to be satisfied. Similarly, the CNT was n type at the positive- V_G onset at V_{G2} in vacuum and at V_{G4} in air, and this should correspond to case (iii). Then the condition $\chi_m > \phi_s + \zeta$ had to be satisfied. Therefore, we had $\chi_m < \phi_s + \zeta$ for a negative V_G and $\chi_m > \phi_s + \zeta$ for a positive V_G , or in other words, V_G was the major mechanism to determine the sign of $\chi_m - (\phi_s + \zeta) = \chi_m - (\phi_s + \zeta_0) + \alpha V_G$. This is possible when the work function difference at $V_G = 0$, $|\chi_m - (\phi_s + \zeta_0)|$, was small enough compared to the band gap E_G in the gold-CNT system. We believe that this was in fact the case and can now assign a band structure including the electrostatic balance in

the transition region for each V_{Gi} onset ($i = 1-4$) in Fig. 2: Figure 6(c) corresponds to V_{G1} , Fig. 6(f) corresponds to V_{G2} , Fig. 6(d) corresponds to V_{G3} , and Fig. 6(g) corresponds to V_{G4} . Because of an obvious relation $\Phi_{Bh} + \Phi_{Be} = \Phi'_{Bh} + \Phi'_{Be} = E_G$, a large positive band bending ϕ_0 at V_{G1} should occur with a small negative band bending ϕ_0 at V_{G2} in vacuum. In air, a small negative band bending ϕ_0 at V_{G3} should occur with a large positive band bending ϕ_0 at V_{G4} . We can clearly see this trend. The experimentally observed Schottky barrier modulation is consistently explained qualitatively.

We next estimate the relevant numerical values. In order to define the negative oxygen charge density, we project the charged oxygen molecules from the rough surface onto a planar gold (111) surface. If $\Gamma_{\text{ox}}\%$ of the gold plane is covered with oxygen molecules, corresponding to Γ_{ox} oxygen molecules per 100 gold atoms, $\sigma_{\text{ox}}/e = -1.86 \times 10^{13} \Gamma_{\text{ox}} \text{ cm}^{-2}$. Then the contribution of σ_{ox} to ΔU is estimated to be $0.251a (\text{\AA}) \Gamma_{\text{ox}}(\%)/\epsilon_{\text{tr}} \text{ eV}$. According to an adsorption experiment of the gold *free* cluster-oxygen molecule system at room temperature, the reaction completion ratio is quite high, larger than 80% (Ref. 21). We can expect a similarly high completion ratio for the *supported* clusters¹⁵ on the Au(111) surface facing the CNT, which is the case of interest. It has to be emphasized that Γ_{ox} is literally the oxygen chemisorption coverage density, but is more directly related to the gold cluster density, given that the reaction completion ratio is high. The gold cluster height b with an attached oxygen molecule is 2–4 \AA (Ref. 15). Thus we expect the transition region width to be $a \sim 3-5 \text{\AA}$. Generally, gases, including oxygen, have a dielectric constant close to unity.² The gold clusters effectively increase the dielectric constant by $1/[1 - b/a]$ multiplied by an appropriate weighting factor (a function of Γ_{ox}), reflecting the partial coverage with clusters.²² Thus we expect $\epsilon_{\text{tr}} \sim 10^0$. Given $a \sim 3-5 \text{\AA}$ and $\epsilon_{\text{tr}} \sim 10^0$, we find that the projected oxygen density Γ_{ox} needs to be at least $(10^{-1} - 10^0)\%$ for $a\Gamma/\epsilon_{\text{tr}}$ to be on the order of unity. Then the contribution of σ_{ox} to ΔU is a few tenths of an electronvolt, which is comparable to a CNT band gap $E_G \sim 0.5 \text{ eV}$ for an example semiconducting (17,0) CNT (Ref. 23), and our present model describes the Schottky barrier modulation appropriately. The projected oxygen density Γ_{ox} or the gold cluster density can be estimated experimentally to test our model.

Case (ii) will occur for an extremely deep metallic work function χ_m as shown in Fig. 6(e). Case (iv) will occur for an extremely shallow metallic work function as shown in Fig. 6(h). In either case, the CNT is locked into the accumulation mode in vacuum, and there is little Schottky barrier modulation. Recently, Ref. 8 has reported CNT FET's with a pre-threshold slope approaching that of a silicon metal-oxide-semiconductor (MOS) FET. The contacts of these CNT FET's are practically Ohmic and are considered to be related to these extreme work function limits.

The Schottky barrier can be modulated if we introduce a charge at the interface between the electrode and CNT. The charge does not have to originate from gas molecules, but can be from any source. A negative charge will lower the

Schottky barrier for holes, and a positive charge will lower the Schottky barrier for electrons. Thus we need a negative charge for p -CNT and a positive charge for n -CNT to create a good Ohmic contact. By choosing electrode metals carefully, we can achieve either case (ii) or (iv). These cases would be preferable in electronics applications, since the contact properties are insensitive to oxidation (more stable), and an Ohmic contact is quite possible in these limits.

VI. SUMMARY

We have presented a model for Schottky barrier modulation under oxidation in the electrode-CNT system. The model considers an appreciable potential drop change in the transition region due to negatively charged oxygen molecules, in contrast to the standard Schottky theory, which does not consider this degree of freedom at all. The gold surface facing the CNT will have clusters, and oxygen molecules are chemisorbed on top of these clusters. Oxidation increases this potential drop and therefore modifies the Schottky barrier. We have explained how high Φ_{Bh} in vacuum and low Φ_{Bh} in air are possible by showing the behavior of the band structures. The electrode, the transition region with negatively charged oxygen molecules, and the CNT are treated equally in our model. The negatively charged oxygen molecules induce a counterbalancing positive charge in both the electrode and CNT. How this charge is divided between σ_m and σ_{NT} is determined by the electrostatics in the transition region. In the gold-CNT system in Ref. 3, the work function difference between the electrode and CNT had to be small, and Schottky barrier modulation was possible for both holes and electrons. Schottky barrier modulation is large when a CNT depletion mode is involved, while modulation is negligible when a CNT accumulation mode is involved. The negative-charge density σ_{ox} corresponding to a coverage of 0.1%–1% of the gold surface is enough to observe the expected Schottky barrier modulation. Finally, we showed that a Schottky barrier can be modulated by intentionally introducing a charge in the transition region, which approach may be useful in achieving a good Ohmic contact.

ACKNOWLEDGMENTS

The author gratefully acknowledges Alessandra Ricca for providing work before publication and discussions and M. Meyyappan and B. Biegel for discussions and a critical review of the manuscript.

APPENDIX: ANALYTICAL SOLUTIONS

If we apply a gate voltage V_G , carriers are induced in the CNT. Then the CNT Fermi level $\zeta = \zeta(V_G)$ and the effective background doping $N_B = N_B(V_G)$ are determined. The electron affinity for a free CNT is ϕ_s . By specifying the electrode material, we know the work function χ_m for a free surface. The transition region width a and its dielectric constant ϵ_{tr} can be determined either theoretically or empirically. Using these quantities, we will express the CNT band bend-

ing as ϕ_0 and the potential drop in the transition region as ΔU . Two positive energies U_{ox} and U_B and the dielectric constant ratio κ are defined by

$$\begin{aligned} U_{ox} &= ea\sigma_{ox}/\epsilon_{tr}, \\ U_B &= e^2 N_B a^2 / 2\epsilon_{NT}, \\ \kappa &= \epsilon_{NT}/\epsilon_{tr}, \end{aligned} \quad (A1)$$

where ϵ_{NT} is the CNT dielectric constant and σ_{ox} is the oxygen density. The p -CNT and n -CNT scenarios are discussed separately.

(i) p -CNT scenario. When $-\chi_m + \phi_s + \zeta \leq U_{ox}$ (accumulation, $\phi_0 > 0$), an ample accumulation charge is available without noticeable band bending. Thus the solution is given by

$$\phi_0 \sim 0^+. \quad (A2)$$

When $-\chi_m + \phi_s + \zeta \geq U_{ox}$ (depletion, $\phi_0 < 0$), Eq. (5) in Sec. III is modified to Eq. (A3) and its solution is given in Eq. (A4) by

$$(-\phi_0) + 2\kappa(U_B|\phi_0|)^{1/2} + \chi_m - \phi_s - \zeta + U_{ox} = 0, \quad (A3)$$

$$(-\phi_0)^{1/2} = [-U_B^{1/2} + (U_B - \chi_m + \phi_s + \zeta - U_{ox})^{1/2}] / \kappa. \quad (A4)$$

(ii) n -CNT scenario. When $-\chi_m + \phi_s + \zeta \geq U_{ox}$ (accumulation, $\phi_0 < 0$), an ample accumulation charge is available without noticeable band bending. Thus the solution is given by

$$\phi_0 \sim 0^-. \quad (A5)$$

When $-\chi_m + \phi_s + \zeta \leq U_{ox}$ (depletion, $\phi_0 > 0$), Eq. (5) is modified to Eq. (A6) and its solution is given in Eq. (A7) by

$$\phi_0 + 2\kappa(U_B\phi_0)^{1/2} - \chi_m + \phi_s + \zeta - U_{ox} = 0, \quad (A6)$$

$$\phi_0^{1/2} = [-U_B^{1/2} + (U_B + \chi_m - \phi_s - \zeta + U_{ox})^{1/2}] / \kappa. \quad (A7)$$

In both scenarios, once ϕ_0 is obtained, ΔU is evaluated by

$$\Delta U(\phi_0) = \chi_m - (\phi_s + \phi_0 + \zeta), \quad (A8)$$

and then the Schottky barrier Φ_{Bh} is given by

$$\Phi_{Bh} = \phi_s + E_G - \chi_m + \Delta U(\phi_0). \quad (A9)$$

When $\sigma_{ox} = 0$, the familiar boundary condition for electric flux density continuity is satisfied at the interface of the transition region and CNT. In fact, using Eq. (A8), we have

$$\begin{aligned}\varepsilon_{\text{tr}}|\Delta U/a| &= [\chi_m - (\phi_s + |\phi_0| + \zeta)]\varepsilon_{\text{tr}}/a \\ &= 2\kappa(U_B|\phi_0|)^{1/2}\varepsilon_{\text{tr}}/a = e(2\varepsilon_{\text{NT}}|\phi_0|N_B)^{1/2},\end{aligned}\quad (\text{A10})$$

where Eqs. (A3) or (A6), with $U_{\text{ox}}=0$, is used at the second equality. The derivative of ϕ_0 along the depletion layer

length l is related to $\sigma_{\text{NT}}(\phi_0)$ and is given with the planar junction theory⁵ by

$$\varepsilon_{\text{NT}}|d\phi_0/dl| = |e\sigma_{\text{NT}}(\phi_0)| = e(2\varepsilon_{\text{NT}}|\phi_0|N_B)^{1/2}. \quad (\text{A11})$$

Thus $\varepsilon_{\text{tr}}|\Delta U/a|$ in the transition region and $\varepsilon_{\text{NT}}|d\phi_0/dl|$ in the CNT are the same and the electric flux density is certainly continuous at the interface.

*NASA Ames Research Center for Nanotechnology (NACNT) and University Affiliated Research Center (UARC). Electronic address: yamada@nas.nasa.gov

¹G. U. Sumanasekera, C. K. W. Adu, S. Fang, and P. C. Eklund, *Phys. Rev. Lett.* **85**, 1096 (2000); K. Bradley, S.-H. Jhi, P. G. Collins, J. H. One, M. L. Cohen, S. G. Louie, and A. Zettl, *ibid.* **85**, 4361 (2000).

²H. Takahashi, *Electromagnetism* (Shokabo, Tokyo, 1959); R. Kubo, *Statistical Mechanics* (North-Holland, New York, 1965).

³V. Derycke, R. Martel, J. Appenzeller, and Ph. Avouris, *Nano Lett.* **1**, 453 (2001); R. Martel, V. Derycke, J. Appenzeller, K. K. Chan, J. Tersoff, and Ph. Avouris, *Phys. Rev. Lett.* **87**, 256805 (2001); S. Heinze, J. Tersoff, R. Martel, V. Derckce, J. Appenzeller, and Ph. Avouris, *ibid.* **89**, 106801 (2002); J. Appenzeller, J. Koch, V. Derycke, R. Martel, S. Wind, and Ph. Avouris, *ibid.* **89**, 126801 (2002).

⁴S. J. Tans, A. R. M. Verschueren, and C. Dekker, *Nature (London)* **393**, 49 (1998); R. Martel, T. Schmidt, H. R. Shea, T. Hertel, and Ph. Avouris, *Appl. Phys. Lett.* **73**, 2447 (1998); C. Zhou, J. Kong, and H. Dai, *ibid.* **76**, 1597 (2000); A. Bachtold, P. Hadley, T. Nakanishi, and C. Dekker, *Science* **294**, 1317 (2001).

⁵S. M. Sze, *Physics of Semiconductor Devices*, 2nd ed. (Wiley, New York, 1981).

⁶T. Yamada, *Appl. Phys. Lett.* **78**, 1739 (2001).

⁷We consider a series connection of an oxide capacitance C_{ox} and a CNT capacitance C_{CNT} between the doped substrate and grounded electrode, and $\alpha = C_{\text{ox}}/[C_{\text{ox}} + C_{\text{CNT}}]$.

⁸In recent CNT FET experiments by A. Javey, H.-S. Kim, M. Brink, Q. Wang, A. Ural, J. Guo, P. McIntyre, P. McEuen, M. Lundstrom, and H. Dai, *Nature Mat.* **1**, 241 (2002); A. Javey, J. Guo, M. Lundstrom, and H. Dai, *Nature (London)* **424**, 654 (2003), the Ohmic contact was achieved by practically eliminating the Schottky barrier through an appropriate choice of electrode material and the adoption of chemical processing for the contact with an optimized transistor geometry.

⁹G. Attard and C. Barnes, *Surfaces*, Oxford Chemistry Primes (Oxford University Press, New York, 1998); A. Zangwill, *Physics at Surfaces* (Cambridge University Press, New York, 1988).

¹⁰J. Bardeen, *Phys. Rev.* **71**, 717 (1947); W. H. Brattain and J. Bardeen, *Bell Syst. Tech. J.* **32**, 1 (1952).

¹¹A. M. Cowley and S. M. Sze, *J. Appl. Phys.* **36**, 3212 (1965); C. Tejedor and M. Schluter, *Phys. Rev. B* **17**, 5044 (1978); J. Tersoff, *Phys. Rev. Lett.* **52**, 465 (1984); *Phys. Rev. B* **30**, 4874 (1984); **32**, 6968 (1985); J. Tersoff and W. A. Harrison, *Phys. Rev. Lett.* **58**, 2367 (1987).

¹²In F. Leonard and J. Tersoff, *Phys. Rev. Lett.* **84**, 4693 (2000), end and side contacts are compared in placing an electrode on a semiconducting CNT. Unique properties are expected in the end contact case, while traditional properties are expected in the side contact case. Here we deal with the latter as shown in Fig. 1, and

the planar junction theory prevails. These contacts are compared for a metallic CNT in J. J. Palacios, A. J. Perez-Jimenez, E. Louis, E. SanFabian, and J. A. Verges, *ibid.* **90**, 106801 (2003).

¹³M. Aguilar, E. Anguiano, J. A. Aznarez, and J. L. Sacedon, *Surf. Sci.* **482–485**, 935 (2001).

¹⁴J. Liu, A. G. Rinzler, H. Dai, J. H. Hafner, R. K. Bradley, P. J. Boul, A. Lu, T. Iverson, K. Shelimov, C. B. Huffman, F. Rodriguez-Marcias, Y.-S. Shon, T. R. Lee, D. T. Colbert, and R. E. Smalley, *Science* **280**, 1253 (1998); L. Liu, T. Wang, J. Li, Z.-X. Guo, L. Dai, D. Zhang, and D. Zhu, *Chem. Phys. Lett.* **367**, 747 (2003).

¹⁵G. Mills, M. S. Gordon, and H. Metiu, *J. Chem. Phys.* **118**, 4198 (2003).

¹⁶D. C. Sorescu, K. D. Jordan, and Ph. Avouris, *J. Phys. Chem.* **105**, 11 227 (2001); A. Ricca and J. A. Dorocco, *Chem. Phys. Lett.* **367**, 217 (2002); A. Ricca, C. W. Bauschlicher, Jr., and A. Maiti, *Phys. Rev. B* **68**, 035433 (2003); P. Giannozzi, R. Car, and G. Scoles, *J. Chem. Phys.* **118**, 1003 (2003).

¹⁷S.-H. Jhi, S. G. Louie, and M. L. Cohen, *Phys. Rev. Lett.* **85**, 1710 (2000); J. Zhao, A. Buldum, J. Han, and J. P. Lu, *Nanotechnology* **13**, 195 (2002).

¹⁸The present model can naturally incorporate a grand canonical situation with fixed electrochemical potentials and is advantageous in electronics applications, while an atomistic *ab initio* model usually handles a canonical situation with a fixed number of electrons.

¹⁹The present model assumes a “fixed” oxygen-CNT distance, but it is straightforward to extend this to the general case with a “distributed” oxygen-CNT distance following the treatment of the MOS flatband voltage-shift problem. Our σ_{ox} simply needs to be replaced by a weighted-average charge [see Eqs. (44)–(46) on pp. 390–395 of Ref. 5]. None of our conclusions change with such a treatment.

²⁰T. Yamada, *Appl. Phys. Lett.* **80**, 4027 (2002).

²¹B. E. Salisbury, W. T. Wallace, and R. L. Whetten, *Chem. Phys.* **262**, 131 (2000).

²²In a parallel-plate capacitor, the capacitance C is given by $C = \varepsilon_0 A/a$, where A is the parallel plate area, a is the parallel plate distance, and ε_0 is the vacuum permittivity. If we insert another metallic plate with thickness b in the gap, the parallel-plate distance is reduced to $a-b$ and $C = \varepsilon_0 A/a[1-b/a]$. This means that the metallic plate increases ε_0 effectively by $1/[1-b/a]$, as described in R. P. Feynman, R. B. Leighton, and M. Sands, *Lectures on Physics* (Addison, Menlo Park, CA, 1964). Similarly, the gold clusters will effectively increase the dielectric constant.

²³M. S. Dresselhaus, G. Dresselhaus, and P. C. Eklund, *Science of Fullerenes and Carbon Nanotubes* (Academic, San Diego, 1996).